



Discovery of 3-(4-bromophenyl)-6-nitrobenzo[1.3.2]dithiazolium ylide 1,1-dioxide as a novel dual cyclooxygenase/5-lipoxygenase inhibitor that also inhibits tumor necrosis factor- α production

Chien-Shu Chen^{a,b}, Chen-Ming Tan^{a,†}, Chiung-Hua Huang^{a,†}, Ling-Chu Chang^c, Jih-Pyang Wang^d, Fong-Chi Cheng^e, Ji-Wang Chern^{a,f,*}

^aSchool of Pharmacy, National Taiwan University, Taipei 100, Taiwan

^bSchool of Pharmacy, China Medical University, Taichung 404, Taiwan

^cInstitute of Medicine, Chung Shan Medical University, Taichung 402, Taiwan

^dDepartment of Education and Research, Taichung Veterans General Hospital, Taichung 407, Taiwan

^eMDS Pharma Services-Taiwan, Taipei 112, Taiwan

^fDepartment of Life Science, National Taiwan University, Taipei 106, Taiwan

ARTICLE INFO

Article history:

Received 7 November 2009

Revised 26 November 2009

Accepted 2 December 2009

Available online 6 December 2009

Keywords:

Virtual screening

Benzo[1.3.2]dithiazolium ylide 1,1-dioxide

Cyclooxygenase

Lipoxygenase

ABSTRACT

In the present study we have discovered compound **1**, a benzo[1.3.2]dithiazolium ylide-based compound, as a new prototype dual inhibitor of cyclooxygenase (COX) and 5-lipoxygenase (5-LOX). Compound **1** was initially discovered as a COX-2 inhibitor, resulting indirectly from the COX-2 structure-based virtual screening that identified compound **2** as a virtual hit. Compounds **1** and **2** inhibited COX-1 and COX-2 in mouse macrophages with IC₅₀ in the range of 1.5–18.1 μ M. Both compounds **1** and **2** were also found to be potent inhibitors of human 5-LOX (IC₅₀ = 1.22 and 0.47 μ M, respectively). Interestingly, compound **1** also had an inhibitory effect on tumor necrosis factor- α (TNF- α) production (IC₅₀ = 0.44 μ M), which was not observed with compound **2**. Docking studies suggested the (*S*)-enantiomer of **1** as the biologically active isomer that binds to COX-2. Being a cytokine-suppressive dual COX/5-LOX inhibitor, compound **1** may represent a useful lead structure for the development of advantageous new anti-inflammatory agents.

© 2009 Elsevier Ltd. All rights reserved.

1. Introduction

Nonsteroidal anti-inflammatory drugs (NSAIDs) such as aspirin, ibuprofen, and indomethacin are widely used for the treatment of pain and inflammation. These drugs block arachidonic acid metabolism by inhibiting the cyclooxygenase (COX) enzymes. The COX enzymes, COX-1 (a constitutive isoform) and COX-2 (an inducible isoform), are responsible for cytoprotective effects and for inflammatory effects, respectively.¹ Classical NSAIDs may cause gastrointestinal (GI) side effects due to indiscriminate inhibition of both COX isoforms.² In recent years, selective COX-2 inhibitors, such as celecoxib,³ rofecoxib,⁴ and valdecoxib⁵ (Chart 1), have been developed as a new generation of NSAIDs with diminished GI side effects. However, rofecoxib and valdecoxib were withdrawn from the market because of an increased risk of cardiovascular complications (e.g., myocardial infarction and stroke).^{6,7} Because COX-2 mediates the biosynthesis of prostacyclin, a vasodilator and inhibitor of platelet aggregation, the inhibition of prostacyclin pro-

duction by selective COX-2 inhibitors might account for their adverse cardiovascular effects.⁸

In addition to the COX pathway, arachidonic acid is also metabolized via the lipoxygenase (LOX) pathway. For example, 5-lipoxygenase (5-LOX) is the key enzyme in the synthesis of leukotrienes from arachidonic acid. Leukotrienes such as LTB₄ are potent mediators of inflammation and allergic reactions.⁹ Thus, 5-LOX inhibitors represent potential therapeutic agents for the treatment of inflammatory and allergic diseases.¹⁰ Recently, dual inhibitors of COX and 5-LOX have emerged as attractive safe alternatives to selective COX-2 inhibitors.¹¹ It has been proposed that inhibition of the COX enzymes by NSAIDs may shunt arachidonic acid metabolism to the 5-LOX pathway.¹² This shunting mechanism leads to increased formation of leukotrienes, which are likely to cause side effects. Early studies suggest that leukotrienes may contribute to the pathogenesis of NSAID-induced GI mucosal damage.¹³ Indeed, increased synthesis of LTB₄ has been found in the gastric mucosa of patients during NSAID treatment.¹⁴ Therefore, dual COX/5-LOX inhibitors can be expected to have a better GI safety profile. A number of dual COX/5-LOX inhibitors have been developed,¹¹ including tepoxalin,¹⁵ tebufelone,¹⁶ and licofelone¹⁷ (Chart 1). Tepoxalin is approved for the treatment of osteoarthritis in dogs in the United

* Corresponding author. Tel.: +886 2 2393 9462; fax: +886 2 2393 4221.

E-mail address: jwchern@ntu.edu.tw (J.-W. Chern).

† These authors contributed equally to this work.

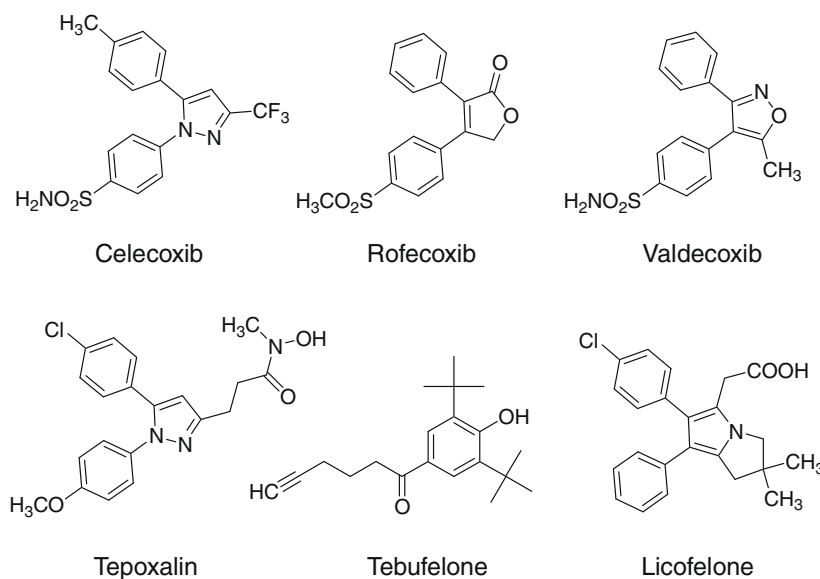


Chart 1. Representative examples of selective COX-2 inhibitors and dual COX/5-LOX inhibitors.

States. Licofelone is the most promising dual COX/5-LOX inhibitor to date that has been evaluated in Phase III clinical trials and shown to be effective in the treatment of osteoarthritis with reduced GI toxicity compared to classical NSAIDs.¹⁸

In this paper, we report the discovery of 3-(4-bromophenyl)-6-nitrobenzo[1.3.2]dithiazolium ylide 1,1-dioxide (**1**, Chart 2) as a novel dual COX/5-LOX inhibitor. Moreover, compound **1** was also found to inhibit the production of tumor necrosis factor- α (TNF- α). The cytokine TNF- α is one of the major mediators of inflammation and has been clinically studied as a therapeutic target for rheumatoid arthritis.¹⁹ Compound **1**, showing multiple effects on the inflammatory processes, may represent a useful lead compound to develop advantageous new anti-inflammatory agents. In this respect, two clinically evaluated dual COX/5-LOX inhibitors, licofelone and S-2474, also displayed cytokine-modulating properties on the production of TNF- α and/or interleukin-1 β (IL-1 β).^{20,21}

To our knowledge, few studies associated with this type of compounds have been reported,^{22–26} and prior to this work the only report on the biological activity of such compounds, including compound **1**, was described by Sang et al.²⁶ This class of compounds was identified as tyrosine kinase inhibitors of the human epidermal growth factor receptor (HER) family (toward HER1, HER2, and HER4). In addition, it should be noted that compound **1** can also be named 1-(4-bromophenyl)-5-nitro-1 λ^4 -benzo[1.3.2]dithiazole 3,3-dioxide, according to the Lambda Convention.

2. Results and discussion

Initially, a structure-based virtual screening approach was used to search for new COX-2 inhibitors.²⁷ The virtual screening was

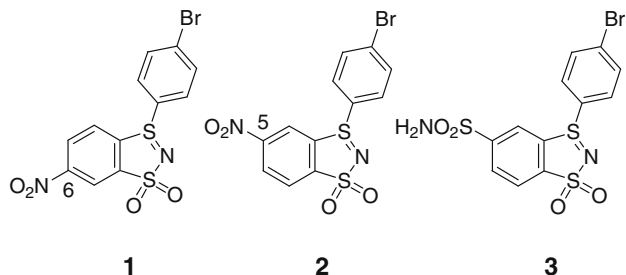


Chart 2. 3-(4-Bromophenyl)benzo[1.3.2]dithiazolium ylide 1,1-dioxides.

performed using the crystal structure of mouse COX-2 bound to SC-558, a COX-2 selective inhibitor (PDB code 6COX).²⁸ The SPECS database (~76,000 commercially available compounds) was computationally screened against the active site of COX-2 using the DOCK 3.5 program.²⁹ The 245 top-scoring compounds were visually inspected for the plausibility of their predicted binding modes, and 17 virtual hits were selected for biological testing. Four of the test compounds showed 21–33% inhibition at 10 μ M against human recombinant COX-2. An encouraging result was obtained with a test compound (SPECS ID number AA-516/31409051, abbreviated here as AA-9051), which exhibited COX-2 inhibition with an IC₅₀ of 1.7 μ M. AA-9051 also inhibited COX-1 derived from human platelets with an IC₅₀ of 6.7 μ M.

The test compound AA-9051 was purchased according to the commercial ID number of the virtual hit compound **2** (Chart 2). This virtual hit was very highly ranked (the fifth) from the DOCK screening. Superimposition of the docking model of compound **2** (as S-form in the database) and the crystal structure of inhibitor SC-558 bound to COX-2 is shown in Figure 1. The *p*-bromophenyl group in both compounds was located in the same hydrophobic pocket. The benzo group of compound **2** was overlaid well with the N1-phenyl ring of SC-558. With respect to polar interactions,

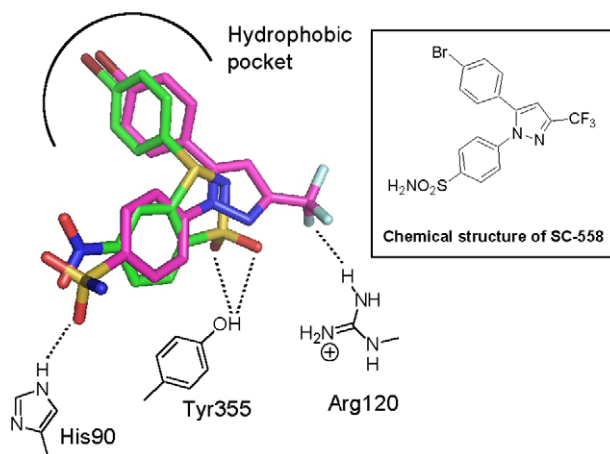


Figure 1. Superimposition of the docking model of compound **2** (S-form, green) and the crystal structure of inhibitor SC-558 (magenta) bound in the active site of COX-2.

the SO₂ group of compound **2** could form two hydrogen bonds with Tyr355. On the other hand, the predicted position of the NO₂ group of compound **2** was not close enough to His90 for hydrogen bond formation. However, the NO₂ group would potentially be expected, like the SO₂ group of SC-558, to form a hydrogen bond with His90 based on the proximity of locations between these two groups and the mobility of the enzyme structure. Taken together, virtual hit **2** became one of the selected compounds for biological testing.

A preliminary study of the structural modification of compound **2** was carried out by replacing the NO₂ group with a SO₂NH₂ group, as seen in SC-558 and celecoxib. The corresponding sulfonamide analog (compound **3**, Chart 2) showed only weak inhibition at 10 μM against human recombinant COX-2 (27% inhibition) and human platelet COX-1 (17% inhibition) (Table 1). Meanwhile, compound **2** (we believed to be AA-9051) was also synthesized in our laboratories. According to the synthetic rationale (Scheme 1), such a route would exclusively produce the desired compound **2**. However, it was surprising that the TLC mobility and ¹H NMR spectrum of the compound prepared were distinct from those of the purchased compound AA-9051. To address this question, the structure of the synthesized compound was analyzed by X-ray crystallography and confirmed to be compound **2** as a racemic mixture (Fig. 2). Accordingly, we concluded that AA-9051 was not identical to compound **2**, and the structural identification of AA-9051 was

mistaken by the chemical supplier. The mass and ¹H NMR analyses of AA-9051 revealed that, compared with compound **2**, this compound had identical molecular weight and showed the same NMR splitting patterns for the three protons of the benzo group. Therefore, we assumed that AA-9051 might be the 6-NO₂ regioisomer of compound **2**, namely compound **1** (Chart 2). Because attempts to produce suitable crystals of AA-9051 for X-ray crystallography failed, we decided to synthesize compound **1** as outlined in Scheme 2 to confirm the above assumption. As expected, the synthesized compound **1** proved to be identical to AA-9051 based on TLC, mass, and ¹H NMR analyses.

Compounds **1** and **2** were evaluated for their ability to inhibit COX-1 and COX-2 using the mouse macrophage cell line RAW 264.7 (Table 2). The data showed that in a cellular environment compound **1** exhibited low micromolar activity against COX-1 (IC₅₀ = 2.1 μM) and COX-2 (IC₅₀ = 4.4 μM). Compound **2** was also a potent inhibitor of COX-1 (IC₅₀ = 1.5 μM); however, it was a four-fold less potent inhibitor of COX-2 (IC₅₀ = 18.1 μM) as compared to compound **1**. The results from cell-based assays indicated that both compounds **1** and **2** are cell membrane permeable and stable in cell culture. The ability of compound **1** to inhibit COX-2 was further assessed in THP-1 cells (a human macrophage cell line). Encouragingly, the anti-COX-2 activity of compound **1** in human THP-1 cells was nearly comparable to that of the reference compound celecoxib (77% vs 83% inhibition at 10 μM).

The emerging trend towards the development of dual COX/5-LOX inhibitors prompted us to test whether compounds **1** and **2** were able to inhibit 5-LOX. In the cell-based assay for human

Table 1
Inhibitory activity of compounds **1–3** on human recombinant COX-2 and human platelet COX-1

Compd	R ₁	R ₂	Inhibitory activity	
			Human recombinant COX-2	Human platelet COX-1
1	H	NO ₂	IC ₅₀ = 1.7 μM	IC ₅₀ = 6.7 μM
2	NO ₂	H	23% @ 10 μM	39% @ 10 μM
3	SO ₂ NH ₂	H	27% @ 10 μM	17% @ 10 μM

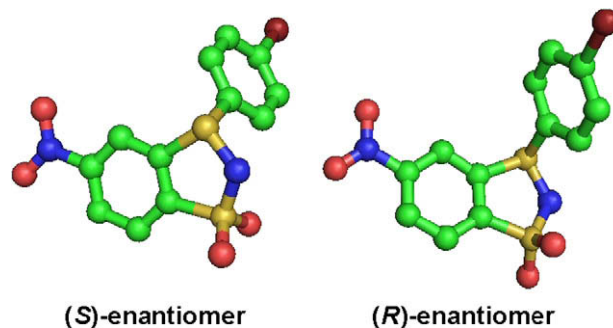
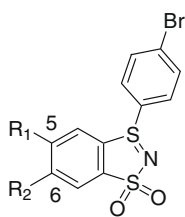
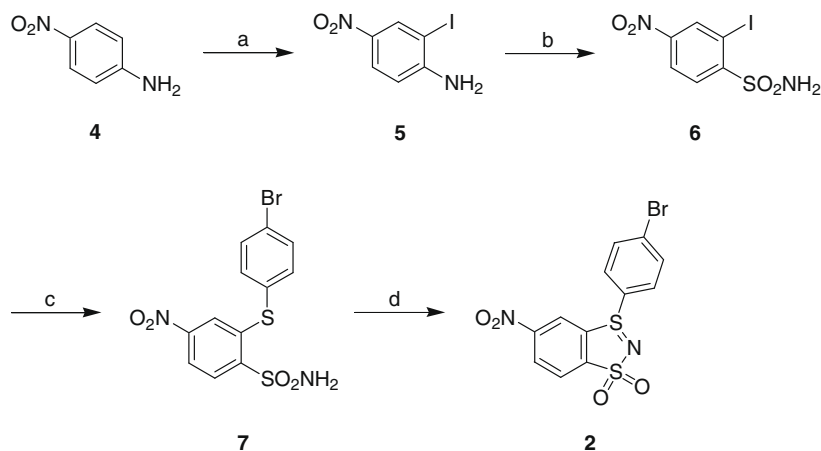
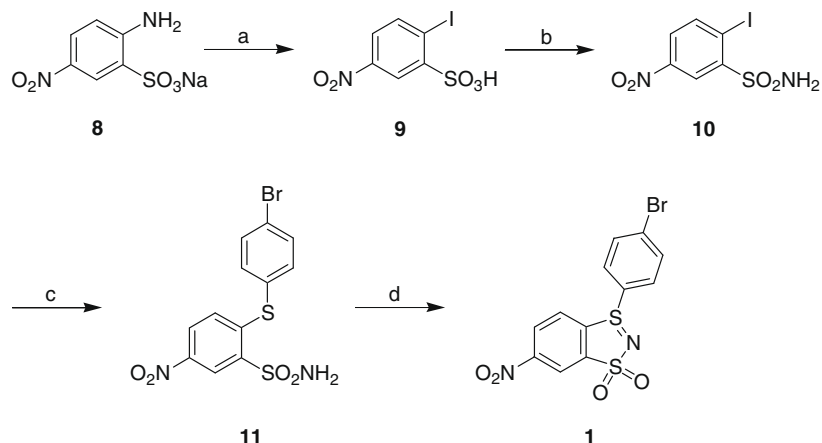


Figure 2. Crystal structures of the (R)- and (S)-enantiomers of compound **2**.



Scheme 1. Synthesis of compound **2**. Reagents and conditions: (a) I₂, Ag₂SO₄, EtOH, room temp, 30 min, 95%; (b) (i) HCl/AcOH, NaNO₂, CH₃CN, <5 °C, 20 min; (ii) SO₂, <7 °C, 40 min, then CuCl₂, room temp, 16 h; (iii) NH₄OH, room temp, 10 h, 22%; (c) 4-bromothiophenol, CuI, neocuproine, *t*-BuONa, toluene, reflux, 8 h, 55%; (d) Br₂, MeOH/H₂O, room temp, 30 min, 56%.



Scheme 2. Synthesis of compound **1**. Reagents and conditions: (a) (i) HCl, NaNO₂, H₂O, 0 °C, 30 min; (ii) KI, room temp, 1 h, 82%; (b) (i) SOCl₂, DMF, reflux, 4 h; (ii) NH₄OH, room temp, 6 h, 60%; (c) 4-bromothiophenol, CuI, neocuproine, *t*-BuONa, toluene, reflux, 8 h, 79%; (d) Br₂, EtOAc/MeOH/H₂O, room temp, 20 min, 54%.

Table 2
Inhibitory activity of compounds **1** and **2** on mouse COXs and human 5-LOX

Compd	R ₁	R ₂	IC ₅₀ (μM)		
			Mouse macrophage ^a		Human leukocyte ^b
			COX-1	COX-2	5-LOX
1	H	NO ₂	2.1	4.4	1.22
2	NO ₂	H	1.5	18.1	0.47
NS-398 ^c			63.7	0.81	—
LM-4108 ^c			56.7	0.21	—

^a Mouse macrophage cell line RAW 264.7.

^b Human peripheral blood mononuclear leukocytes (PBML).

^c COX-2-selective reference compounds used in the assays.

5-LOX in peripheral blood mononuclear leukocytes (PBML), compound **1** exhibited 5-LOX inhibitory activity with an IC₅₀ value of 1.22 μM (Table 2). The 5-NO₂ analog **2** was 2.6-fold more effective in inhibiting 5-LOX (IC₅₀ = 0.47 μM) than compound **1**. Compound **1**, but not compound **2**, was considered a lead structure for future optimization because this compound was shown to be a relatively potent COX-2 inhibitor and possess an additional anti-inflammatory pharmacological activity related to inhibition of TNF-α production as discussed below.

Compounds **1** and **2** were tested for their effects on TNF-α production from LPS-stimulated human THP-1 macrophages. Compound **1** inhibited TNF-α production by 92% at 10 μM, whereas compound **2** lacked such biological activity (Fig. 3A). As shown in Figure 3B, there was a concentration-dependent suppression of TNF-α production by compound **1** with an IC₅₀ of 0.44 μM. The COX-2 selective drug celecoxib, also tested in this assay, showed no effect on TNF-α production. It has been pointed out that NSAIDs, generally considered anti-inflammatory, might also be pro-inflammatory by increasing TNF-α levels.³⁰ For example, aspirin,³¹ ibuprofen,³² indomethacin,³³ and rofecoxib³⁴ have been demonstrated to up-regulate TNF-α production. Moreover, it has been suggested that TNF-α plays a critical role in NSAID-induced gastric mucosal injury.³³ Because compound **1** could inhibit TNF-α

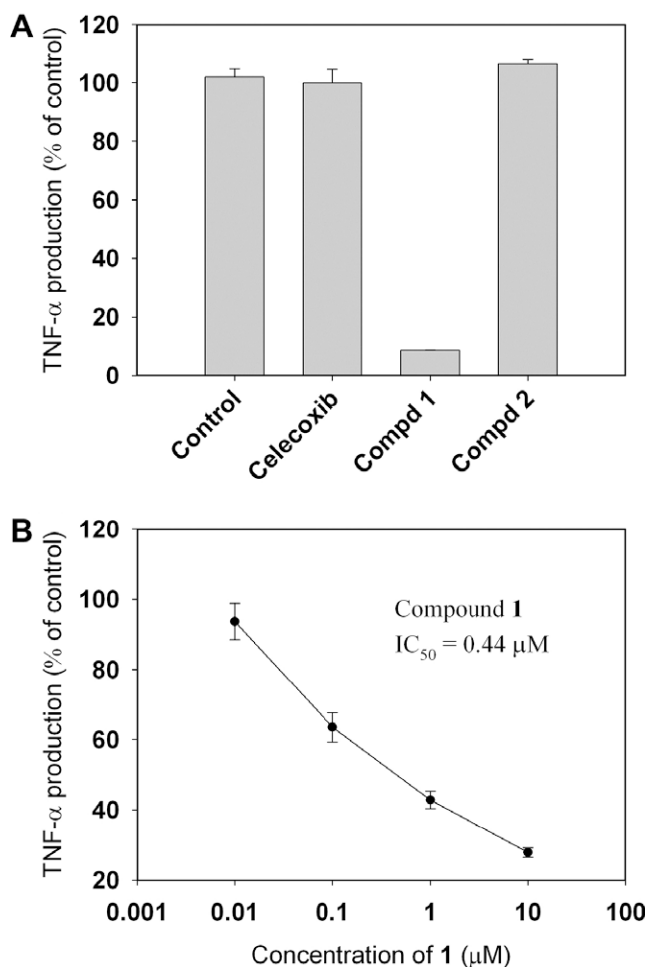


Figure 3. (A) Effect of compounds **1** and **2**, and celecoxib (10 μM) on TNF-α production in LPS-stimulated THP-1 cells. The positive control, dexamethasone, was tested at 1 μM, showing 89% inhibition of TNF-α production. Data represent the mean ± SD of duplicate determinations. (B) Concentration-dependent inhibition of TNF-α production by compound **1** in THP-1 cells. Data represent the mean ± SD of duplicate determinations.

production, it not only would be devoid of these potential side effects but was also expected to have greater anti-inflammatory efficacy through combination with COX/5-LOX inhibition. The inhibition mechanism of compound **1** on TNF-α production remains to

be elucidated, and a possibility through inhibition of p38 kinase³⁵ could be ruled out based on our study, showing no inhibition of p38 α kinase by compound **1** at 10 μ M.

To predict the binding mode of compound **1** in the COX-2 active site, docking studies were carried out using the program GOLD (version 3.1.1).³⁶ The GOLD program can perform flexible ligand docking simulations and thus may allow better prediction of the binding mode for a compound when compared with the DOCK 3.5 program used in the virtual screening, which performs rigid-body ligand docking using only a single conformation. In addition, it was possible that differences in the conformations of active site residues might be present in the different crystal structures of COX-2 (free and in complex with various inhibitors). We therefore attempted to utilize several reported crystal structures of COX-2 for docking simulations in order to find one that would create the most favorable interactions with compound **1**. The four crystal structures used in the docking studies include mouse COX-2 unliganded (PDB code 5COX) and complexed with inhibitors flurbiprofen, indomethacin, and SC-558 (PDB codes 3PGH, 4COX, and 6COX, respectively).²⁸

Because compound **1** contains a chiral sulfur atom and exists as a racemate, we sought to predict which enantiomer might be the biologically active form through the docking studies. Docking studies were first performed on the (*S*)-enantiomeric form of compound **1** ((*S*)-**1**) in the active site of the four COX-2 crystal structures because the (*S*)-enantiomeric form of compound **2** was initially identified in the virtual screening. The docking solutions of (*S*)-**1** obtained using the crystal structures 3PGH, 4COX, 5COX, and 6COX had GOLD fitness scores of 40.82, 48.20, 46.55, and 44.04, respectively. The predicted binding orientations of (*S*)-**1** were similar when docked into the crystal structures 4COX, 5COX, and 6COX. On the other hand, the docking solution obtained using the crystal structure 3PGH was eliminated because (*S*)-**1** was located outside the ligand-binding site. The docking solution for (*S*)-**1** that demonstrated the highest GOLD fitness score (48.20 for 4COX) was chosen to represent the predicted binding mode to COX-2 (Fig. 4). As indicated in Figure 4, (*S*)-**1** formed two hydrogen bonds via the SO₂ group with Arg120 (3.4 Å) and Tyr355 (2.5 Å). Similar interactions were observed from the carboxylate group of indomethacin with the COX-2 enzyme (4COX structure). In addition, the NO₂ group of (*S*)-**1** was inserted into the side pocket of COX-2 and formed two hydrogen bonds with His90 (3.0 Å) and

Arg513 (3.1 Å). The NO₂ group in compound **1** was shown to be important for inhibiting COX-2 because the corresponding 6-desnitro analog displayed no inhibition at 10 μ M against human recombinant COX-2.

We subsequently carried out the docking study of (*R*)-**1** enantiomer with the crystal structure 4COX. The docking solution of (*R*)-**1** had a lower GOLD fitness score than that of (*S*)-**1** (42.50 vs 48.20). The two enantiomeric forms were predicted to interact with COX-2 in a completely different manner. It was observed that instead of the *p*-bromophenyl moiety, the bicyclic heterocycle of (*R*)-**1** occupied the hydrophobic pocket and formed two hydrogen bonds via the SO₂ group with Tyr385 and Ser530 (Fig. 5). However, the polar NO₂ group of (*R*)-**1** appeared to be unfavorably located because it did not make any hydrogen bonds and had unfavorable contacts with the nonpolar side chains of surrounding residues. These results contradicted the importance of the role of the NO₂ group in compound **1** as an inhibitor of COX-2. Taken together, it was hypothesized that (*S*)-**1** would be the biologically active enantiomer against COX-2.

3. Conclusions

In conclusion, through structure-based virtual screening, structural identification, and biological evaluations, we ultimately determined that compound **1** is a novel dual COX/5-LOX inhibitor as well as an inhibitor of TNF- α production. Compound **1**, showing multiple actions on the inflammatory pathways, may represent a useful lead compound for the development of new anti-inflammatory agents that would have a better GI safety profile and a broad spectrum of anti-inflammatory activities. Further studies on the structural modifications of this compound are currently underway.

4. Experimental

4.1. Virtual screening

The X-ray crystal structure of mouse COX-2 (PDB code 6COX) was retrieved from the Protein Data Bank (<http://www.rcsb.org/pdb>) to prepare the target site for docking calculations. The B-chain structure of protein and small molecules were removed. The remaining

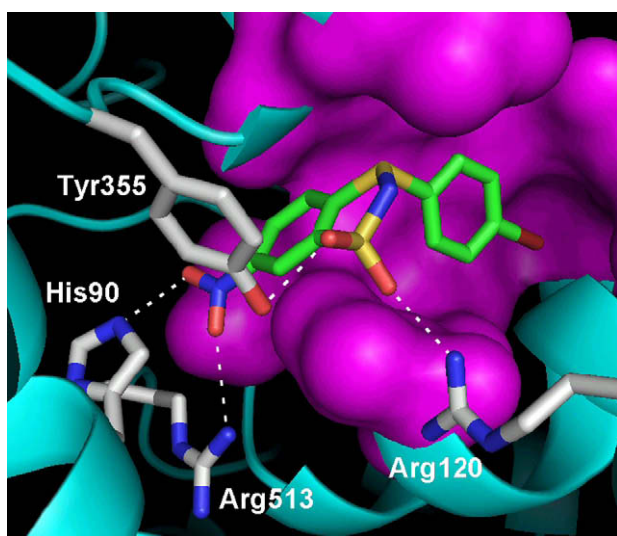


Figure 4. Predicted binding mode of the (*S*)-enantiomer of compound **1** in the active site of COX-2. The dashed lines indicate hydrogen bonds. The hydrophobic pocket is represented as a molecular surface (magenta).

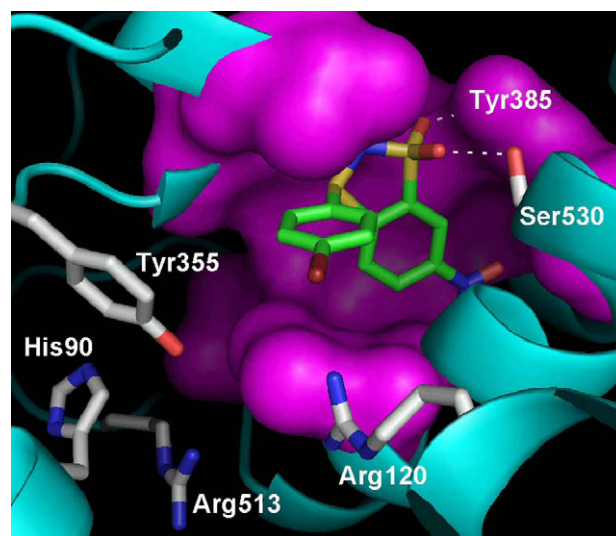


Figure 5. Docking model of the (*R*)-enantiomer of compound **1** in the active site of COX-2. The dashed lines indicate hydrogen bonds. The hydrophobic pocket is represented as a molecular surface (magenta).

A-chain protein structure was used for the virtual screening performed with the DOCK 3.5 program. The active site region of COX-2 was specified as the target site for ligand docking in virtual screening. Briefly, a molecular surface around the target site was generated with the MS program using a 1.4 Å probe radius, and this surface was used to generate with the SPHGEN program 44 overlapping spheres to fill the target site. A grid box enclosing the target site was created for grid calculations with dimensions 21.2 × 13.8 × 18.5 Å. The force field scoring grids were calculated with the CHEMGRID program using default AMBER parameters, a distance-dependent dielectric constant of 4r, close contact limits of 2.3 and 2.8 Å for receptor polar and nonpolar atoms, respectively, a nonbonded cutoff of 10 Å, and a grid spacing of 0.3 Å. The database for virtual screening was the SPECS compound collection (2002 release, <http://www.specs.net>), which included approximately 76,000 compounds. The three-dimensional structures of the SPECS compounds were generated using the CONCORD program (Tripos, Inc., St. Louis, MO). The DOCK 3.5 program performed rigid-body docking using a distance-matching algorithm. The matching parameters used to run virtual screening were set as follows: distance_tolerance = 1.5, nodes_maximum = 8, nodes_minimum = 4, ligand_binsize = 0.4, ligand_overlap = 0.1, receptor_binsize = 0.4, receptor_overlap = 0.1, and bump_maximum = 0. The SPECS database was computationally screened against the active site of COX-2 using the force field scoring function based on interaction energy. Virtual screening was performed on a Silicon Graphics Octane workstation with dual 270 MHz MIPS R12000 processors.

For compound selection, the docking models of the 245 top-ranked compounds (energy scores ranging from –69.2 to –37.8 kcal/mol) were visually inspected using the software Insight II (Accelrys Inc., San Diego, CA). Together with consideration of chemical diversity, the selection of compounds was assisted by visual analysis of the docking models with respect to shape fitting and hydrogen-bonding and hydrophobic interactions. Finally, we selected 17 compounds for COX-2 inhibition assay. The compounds for testing were purchased from the SPECS company. The SPECS ID numbers for compounds are listed as follows: AA-516/31409051 (compound **1**), AG-205/37204019, AC-907/34122064, AG-205/12145002, AG-205/36628044, AK-968/12686132, AG-205/12368031, AE-848/34434063, AG-205/33120044, AG-690/34549025, AK-968/11109006, AF-399/36911008, AF-615/30368003, AG-205/3368050, AK-660/36747022, AG-227/37195079, AG-690/34649013.

4.2. Molecular docking studies

Four crystal structures of mouse COX-2 (PDB codes: 3PGH, 4COX, 5COX, and 6COX) were used for docking studies of compound **1**. For each crystal structure, the A-chain protein structure with hydrogen atoms added was utilized in the docking experiments. The 3-D structures of (*S*)-**1** and (*R*)-**1** enantiomers were built and optimized by energy minimization using the Tripos force field in the software package SYBYL 6.5 (Tripos, Inc., St. Louis, MO). Docking experiments were performed using the GOLD program (version 3.1.1) on a Silicon Graphics Octane workstation with dual 270 MHz MIPS R12000 processors. The GOLD program utilizes a genetic algorithm (GA) to perform flexible ligand docking simulations. In the present study, for each of the 30 independent GA runs, a maximum number of 100,000 GA operations were performed on a single population of 100 individuals. Operator weights for crossover, mutation, and migration were set to 95, 95, and 10, respectively. Default cutoff values of 2.5 Å for hydrogen bonds and 4.0 Å for van der Waals distance were used. The GoldScore fitness function was applied for scoring the docking poses using EXTERNAL_ENERGY_WT = 1.0. Firstly, (*S*)-**1** enantiomer was studied for docking into each active site of the four COX-2 crystal structures. The docking solutions obtained using the crystal structures

3PGH, 4COX, 5COX, and 6COX had GOLD fitness scores of 40.82, 48.20, 46.55, and 44.04, respectively. The docking solution for (*S*)-**1** that demonstrated the highest score (48.20 for 4COX) was chosen to represent the predicted binding mode to COX-2 (Fig. 4). The crystal structure 4COX was then used in the docking study of (*R*)-**1** enantiomer. The top-ranked docking model of (*R*)-**1** (GOLD fitness score: 42.50) is shown in Figure 5.

4.3. Chemistry

4.3.1. Synthesis of 3-(4-bromophenyl)-5-nitrobenzo[1.3.2]dithiazolium ylide 1,1-dioxide (**2**)

4.3.1.1. 2-Iodo-4-nitroaniline (5**).** 4-Nitroaniline (**4**, 5.43 g) was added to a mixture of iodine (10 g) and Ag₂SO₄ (12.24 g) in EtOH (100 mL), and the mixture was stirred at room temperature for 30 min. The reaction mixture was filtered, and the filtrate was evaporated under reduced pressure. The resulting residue was dissolved in CH₂Cl₂, washed with 5% NaOH and H₂O, dried (MgSO₄), and evaporated to dryness to give **5** as a yellow solid (95% yield). Mp 106–107 °C (lit. 107 °C³⁷). ¹H NMR (200 MHz, acetone-*d*₆) δ 8.44 (d, *J* = 2.4 Hz, 1H, ArH), 7.99 (dd, *J* = 2.4, 9 Hz, 1H, ArH), 6.88 (d, *J* = 9 Hz, 1H, ArH), 6.13 (s, 2H, NH₂). ¹³C NMR (50 MHz, acetone-*d*₆) δ 154.60, 138.47, 135.66, 125.91, 112.77, 79.58.

4.3.1.2. 2-Iodo-4-nitrobenzenesulfonamide (6**).** To a solution of compound **5** (5.28 g, 20 mmol) in CH₃CN (150 mL) cooled to a temperature <5 °C in an ice bath were added concd HCl (16 mL) and AcOH (8 mL). A solution of NaNO₂ (1.66 g) in H₂O (3 mL) was then added slowly via syringe to the acidic solution. After complete addition, the mixture was stirred for 20 min. SO₂ gas was bubbled into the mixture at a temperature <7 °C for 40 min. To the resulting mixture was then added a solution of anhydrous CuCl₂ (3.4 g, 25 mmol) in H₂O (3 mL). When the mixture became deep brown, the ice bath was removed, and stirring was continued at room temperature for 16 h. The reaction mixture was concentrated to a small volume and poured into ice water. The yellow solid was collected by filtration to give the sulfonyl chloride derivative. The sulfonyl chloride compound was treated with excess ammonia water in an ice bath, and the mixture was allowed to stir at room temperature for 10 h. The mixture was concentrated to a small volume, extracted with EtOAc and CHCl₃, and evaporated to dryness. Purification of the crude product by flash column chromatography (hexane) gave **6** in 22% yield. Mp 203 °C. ¹H NMR (400 MHz, acetone-*d*₆) δ 8.84 (d, *J* = 2.4 Hz, 1H, ArH), 8.42 (dd, *J* = 8.8, 2.4 Hz, 1H, ArH), 8.36 (d, *J* = 8.8 Hz, 1H, ArH), 7.04 (s, 2H, SO₂NH₂). ¹³C NMR (100 MHz, acetone-*d*₆) δ 152.03, 149.72, 137.56, 130.64, 124.12, 92.38. MS (EI) *m/z* = 328 [M]⁺. Anal. Calcd for C₆H₅IN₂O₄S: C, 21.97; H, 1.54; N, 8.54. Found: C, 21.88; H, 1.46; N, 8.55.

4.3.1.3. 2-(4-Bromophenylsulfanyl)-4-nitrobenzenesulfonamide (7**).** To a mixture of aryl iodide **6** (0.2 g), CuI (0.014 g), neocuproine (0.016 g), and *t*-BuONa (0.126 g) in toluene was added 4-bromothiophenol (0.14 g). The mixture was refluxed under N₂ for 8 h. The reaction mixture was neutralized with dil HCl and then evaporated under reduced pressure. The resulting residue was extracted with EtOAc (3 × 15 mL), and the extracts were evaporated to dryness. The crude product was purified by flash column chromatography (hexane/EtOAc 1:1) to give **7** in 55% yield. ¹H NMR (200 MHz, acetone-*d*₆) δ 8.20 (m, 2H, ArH), 7.83 (d, *J* = 2 Hz, 1H, ArH), 7.72 (m, 2 H, ArH), 7.60 (m, 2H, ArH), 7.12 (s, 2H, SO₂NH₂). ¹³C NMR (50 MHz, acetone-*d*₆) δ 150.48, 146.36, 140.17, 137.01, 133.99, 131.65, 130.43, 125.08, 124.53, 121.34.

4.3.1.4. 3-(4-Bromophenyl)-5-nitrobenzo[1.3.2]dithiazolium ylide 1,1-dioxide (2**).** To a solution of **7** (0.06 g) in MeOH/H₂O (6 mL/2 mL) was added bromine (0.015 mL, 0.045 g). The mixture was

stirred at room temperature for 30 min. The precipitated solid was collected by filtration, washed with H₂O, and recrystallized from acetone/hexane to give product **2** in 56% yield. Mp 294–296 °C. ¹H NMR (400 MHz, acetone-*d*₆) δ 9.09 (d, *J* = 1.84 Hz, 1H, ArH), 8.77 (dd, *J* = 8.4, 1.84 Hz, 1H, ArH), 8.32 (d, *J* = 8.4 Hz, 1H, ArH), 7.97 (dd, *J* = 6.7, 2 Hz, 2H, ArH), δ 7.82 (dd, *J* = 6.7, 2 Hz, 2H, ArH). ¹³C NMR (100 MHz, acetone-*d*₆) δ 151.84, 141.51, 137.73, 137.53, 137.08, 134.11, 130.28, 128.43, 124.97, 122.75. MS (EI) *m/z* = 388 [M+2]⁺. Anal. Calcd for C₁₂H₇BrN₂O₄S₂: C, 37.22; H, 1.82; N, 7.23. Found: C, 37.30; H, 2.44; N, 7.13.

4.3.2. Synthesis of 3-(4-bromophenyl)-6-nitrobenzo[1.3.2]dithiazolium ylide 1,1-dioxide (1)

4.3.2.1. 2-Iodo-5-nitrobenzenesulfonic acid (9). 2-Amino-5-nitrobenzenesulfonic acid, sodium salt (**8**, 5 g) was dissolved in H₂O (150 mL). To this solution cooled in an ice bath were added a solution of NaNO₂ (1.72 g) in H₂O (5 mL) and concd HCl (5 mL). After stirring at 0 °C for 30 min, KI (4.15 g) was added to the mixture. The ice bath was removed, and the mixture was allowed to stir at room temperature for 1 h. The reaction mixture was concentrated to a small volume, and the solid was collected by filtration to give **9** in 82% yield. ¹H NMR (400 MHz, DMSO-*d*₆) δ 8.58 (d, *J* = 2.8 Hz, 1H, ArH), 8.18 (d, *J* = 8.4 Hz, 1H, ArH), 7.81 (dd, *J* = 8.4, 2.8 Hz, 1H, ArH); ¹³C NMR (100 MHz, DMSO-*d*₆) δ 151.85, 146.88, 142.69, 123.97, 121.85, 103.00.

4.3.2.2. 2-Iodo-5-nitrobenzenesulfonamide (10). A mixture of **9** (3.5 g), thionyl chloride (20 mL), and DMF (0.4 mL) was refluxed for 4 h. The reaction mixture was evaporated under reduced pressure, and the residue was then evaporated from toluene (5 mL) to remove residual thionyl chloride. To the sticky residue cooled in an ice bath was added ammonia water (30 mL) in portions. After stirring at room temperature for 6 h, the reaction mixture was concentrated to a small volume and then extracted with EtOAc (3 × 20 mL). The extracts were evaporated, and the residue was purified by flash column chromatography (hexane/EtOAc 1:1) to give **10** in 60% yield. Mp 187 °C. ¹H NMR (200 MHz, acetone-*d*₆) δ 8.78 (d, *J* = 2.6 Hz, 1H, ArH), 8.44 (d, *J* = 8.4 Hz, 1H, ArH), 8.07 (d, *J* = 8.4, 2.6 Hz, 1H, ArH), 7.06 (s, 2H, SO₂NH₂). ¹³C NMR (50 MHz, acetone-*d*₆) δ 170.50, 147.99, 144.63, 126.95, 123.61, 100.86. MS (EI) *m/z* = 328 [M]⁺. Anal. Calcd for C₆H₅IN₂O₄S: C, 21.97; H, 1.54; N, 8.54. Found: C, 21.79; H, 1.50; N, 8.49.

4.3.2.3. 2-(4-Bromophenylsulfanyl)-5-nitrobenzenesulfonamide (11). To a mixture of aryl iodide **10** (0.2 g), CuI (0.014 g), neocuproine (0.016 g), and *t*-BuONa (0.126 g) in toluene was added 4-bromothiophenol (0.14 g). The mixture was refluxed under N₂ for 8 h. The reaction mixture was neutralized with dil HCl and then evaporated under reduced pressure. The resulting residue was extracted with EtOAc (3 × 15 mL), and the extracts were evaporated to dryness. The crude product was purified by flash column chromatography (hexane/EtOAc 1:1) to give **11** in 79% yield. ¹H NMR (200 MHz, acetone-*d*₆) δ 8.73 (d, *J* = 2.6 Hz, 1H, ArH), 8.23 (dd, *J* = 8.8, 2.6 Hz, 1H, ArH), 7.74 (m, 2 H, ArH), 7.60 (m, 2H, ArH), 7.25 (d, *J* = 8.8 Hz, 1H, ArH), 7.09 (s, 2H, SO₂NH₂). ¹³C NMR (50 MHz, acetone-*d*₆) δ 147.02, 145.68, 141.60, 137.79, 134.23, 130.71, 127.05, 125.13, 123.98, 110.29.

4.3.2.4. 3-(4-Bromophenyl)-6-nitrobenzo[1.3.2]dithiazolium ylide 1,1-dioxide (1). To a solution of **11** (0.1 g) in EtOAc/MeOH/H₂O (11 mL/10 mL/3 mL) was added bromine (0.008 mL, 0.025 g). The mixture was stirred at room temperature for 20 min and poured into H₂O (50 mL). The precipitated solid was collected by filtration, washed with H₂O, and purified by flash column chromatography (hexane/EtOAc 2:3) to give product **1** in 54% yield. Mp 246 °C. ¹H NMR (400 MHz, acetone-*d*₆) δ 8.74 (d, *J* = 1.7 Hz, 1H, ArH), 8.70

(dd, *J* = 8.6, 1.7 Hz, 1H, ArH), 8.48 (d, *J* = 8.6 Hz, 1H, ArH), 7.95 (d, *J* = 8.7 Hz, 2H, ArH), 7.82 (d, *J* = 8.7 Hz, 2H, ArH). ¹³C NMR (100 MHz, acetone-*d*₆) δ 140.90, 138.82, 137.81, 134.22, 130.16, 129.42, 128.52, 128.32, 119.14, 116.69. MS (EI) *m/z* = 388 [M+2]⁺. Anal. Calcd for C₁₂H₇BrN₂O₄S₂: C, 37.22; H, 1.82; N, 7.23. Found: C, 37.18; H, 2.08; N, 7.62.

4.4. Human COX-2 and COX-1 inhibition assays

The human COX inhibition assays were performed by MDS Pharma Services (Taipei, Taiwan) using the test methods numbered 118010 and 116020 for COX-2 and COX-1, respectively. The enzyme sources for COX-2 and COX-1 were human recombinant COX-2 (expressed in insect Sf21 cells) and human platelets, respectively.

4.4.1. Human COX-2 inhibition assay

Test compounds were preincubated for 15 min at 37 °C with purified human recombinant COX-2 (0.11 U) in Tris–HCl buffer (pH 7.7) containing glutathione (1 mM), phenol (500 μM), and hematin (1 μM). The enzymatic reaction was initiated by addition of 0.3 μM arachidonic acid. After 5 min incubation at 37 °C, the reaction was terminated by addition of 1 N HCl. Prostaglandin E₂ (PGE₂) production was quantified to measure COX-2 activity using an enzyme immunoassay (EIA) kit (Amersham).

4.4.2. Human COX-1 inhibition assay

Test compounds were preincubated for 15 min at 37 °C with human platelets (5 × 10⁷ cells/mL) in modified HEPES buffer (pH 7.4). The enzymatic reaction was initiated by addition of 100 μM arachidonic acid. After 15 min incubation at 37 °C, the reaction was terminated by addition of 1 N HCl. PGE₂ production was quantified to measure COX-1 activity using an EIA kit.

4.5. Macrophage COX-1 and COX-2 inhibition assays using mouse RAW 264.7 cells

For macrophage COX-1 and COX-2 assays, mouse RAW 264.7 cells (5 × 10⁵ cells) in 0.5 mL of DMEM supplemented with 10% heat-inactivated fetal bovine serum (FBS), 100 U/mL penicillin, and 100 μg/mL streptomycin were seeded in a 24-well culture plate and grown at 37 °C under an atmosphere of 5% CO₂ overnight. Cells were washed with phosphate buffered saline (PBS, pH 7.2) twice. At this stage, in the case of COX-2 assay, the cells were then stimulated with 1 μg/mL LPS (serotype 0111:B4) in DMEM medium for 6 h and were washed again with PBS twice. The culture medium was replaced by DMEM medium without phenol red and FBS, and then cells were pretreated with test compounds for 1 h at 37 °C before the addition of 30 μM arachidonic acid. After 30 min incubation at 37 °C, the medium was collected for PGE₂ assay using a PGE₂ EIA kit according to the manufacturer's instructions.

4.6. Assay of human 5-LOX inhibition

The human 5-LOX inhibition assay was performed by MDS Pharma Services (Taipei, Taiwan) using the test method numbered 136,010. The 5-LOX source was human peripheral blood mononuclear leukocytes (PBML). Test compounds were preincubated for 15 min at 37 °C with human PBML (5 × 10⁶ cells/mL) in HBSS buffer (pH 7.4). The enzymatic reaction was initiated by addition of the calcium ionophore A23187 (30 μM). After 15 min incubation at 37 °C, the reaction was terminated by addition of 1 N HCl. After neutralization with NaOH and centrifugation, the LTB₄ concentration in the supernatant was measured using an EIA kit.

4.7. Assay for inhibition of TNF- α production in THP-1 cells

The human monocytic THP-1 cells (ATCC No. TIB-202) were grown in RPMI-1640 medium supplemented with 10% FBS, 4.5 μ g/L glucose, 10 mM HEPES, 1.0 mM sodium pyruvate, penicillin (100 U/mL), streptomycin (0.1 mg/mL), amphotericin B (0.25 μ g/mL), and L-glutamine (2 mM) at 37 °C in humidified 5% CO₂. To prepare conditioned medium for the differentiation of THP-1 cells into macrophages, THP-1 cells (1–2 \times 10⁷ cells/mL) in RPMI-1640 medium supplemented with 10% FBS were treated with 200 ng/mL phorbol myristate acetate (PMA, Sigma, USA) for 24 h at 37 °C in humidified 5% CO₂, washed three times with PBS, and incubated for another 24 h to eliminate the effect of PMA. For TNF- α release assay, THP-1 cells were stimulated with the conditioned medium in a 96-well plate for 72 h to differentiate into macrophages. The differentiated THP-1 cells were preincubated with test compounds at various concentrations (0.01, 0.1, 1, and 10 μ M) for 1 h at 37 °C. The cells were then stimulated with 100 ng/mL LPS (Sigma, USA) for 24 h. Cell-free supernatants were collected, and TNF- α levels were determined using a commercial ELISA kit (Biosource, cat. no. KHC3012).

Acknowledgments

This work was supported by the National Science Council of the Republic of China (Grants NSC94-2320-B002-097, NSC95-2320-B002-035, and NSC96-2320-B002-017). We thank Taiwan Biotech Co., Ltd. for the gift of celecoxib. Current address for Chien-Shu Chen is China Medical University.

References and notes

- Hla, T.; Neilson, K. *Proc. Natl. Acad. Sci. U.S.A.* **1992**, *89*, 7384.
- Cryer, B.; Feldman, M. *Am. J. Med.* **1998**, *104*, 413.
- Penning, T. D.; Talley, J. J.; Bertenshaw, S. R.; Carter, J. S.; Collins, P. W.; Docter, S.; Graneto, M. J.; Lee, L. F.; Malecha, J. W.; Miyashiro, J. M.; Rogers, R. S.; Rogier, D. J.; Yu, S. S.; Anderson, G. D.; Burton, E. G.; Cogburn, J. N.; Gregory, S. A.; Koboldt, C. M.; Perkins, W. E.; Seibert, K.; Veenhuizen, A. W.; Zhang, Y. Y.; Isakson, P. C. *J. Med. Chem.* **1997**, *40*, 1347.
- Prasit, P.; Wang, Z.; Brideau, C.; Chan, C. C.; Charleson, S.; Cromlish, W.; Ethier, D.; Evans, J. F.; Ford-Hutchinson, A. W.; Gauthier, J. Y.; Gordon, R.; Guay, J.; Gresser, M.; Kargman, S.; Kennedy, B.; Leblanc, Y.; Leger, S.; Mancini, J.; O'Neill, G. P.; Ouellet, M.; Percival, M. D.; Perrier, H.; Riendeau, D.; Rodger, I.; Zamboni, R., et al. *Bioorg. Med. Chem. Lett.* **1999**, *9*, 1773.
- Talley, J. J.; Brown, D. L.; Carter, J. S.; Graneto, M. J.; Koboldt, C. M.; Masferrer, J. L.; Perkins, W. E.; Rogers, R. S.; Shaffer, A. F.; Zhang, Y. Y.; Zweifel, B. S.; Seibert, K. *J. Med. Chem.* **2000**, *43*, 775.
- Dogne, J. M.; Supuran, C. T.; Pratico, D. *J. Med. Chem.* **2005**, *48*, 2251.
- Solomon, D. H. *Arthritis Rheum.* **2005**, *52*, 1968.
- McAdam, R. F.; Catella-Lawson, F.; Nardini, I. A.; Fitzgerald, G. A. *Proc. Natl. Acad. Sci. U.S.A.* **1999**, *96*, 272.
- Lewis, R. A.; Austen, K. F.; Soberman, R. J. *N. Eng. J. Med.* **1990**, *323*, 645.
- Jampilek, J.; Dolezal, M.; Opletalova, V.; Hartl, J. *Curr. Med. Chem.* **2006**, *13*, 117.
- (a) Kulkarni, S. K.; Singh, V. P. *Inflammopharmacology* **2008**, *16*, 1; (b) Leone, S.; Ottani, A.; Bertolini, A. *Curr. Top. Med. Chem.* **2007**, *7*, 265; (c) Charlier, C.; Michaux, C. *Eur. J. Med. Chem.* **2003**, *38*, 645.
- Martel-Pelletier, J.; Lajeunesse, D.; Reboul, P.; Pelletier, J. P. *Ann. Rheum. Dis.* **2003**, *62*, 501.
- Rainsford, K. D. *Agents Actions* **1993**, *39*, C24.
- Hudson, N.; Balsitis, M.; Everitt, S.; Hawkey, C. J. *Gut* **1993**, *34*, 742.
- Argentieri, D. C.; Ritchie, D. M.; Ferro, M. P.; Kirchner, T.; Wachter, M. P.; Anderson, D. W.; Rosenthal, M. E.; Capetola, R. J. *J. Pharmacol. Exp. Ther.* **1994**, *271*, 1399.
- Weisman, S. M.; Doyle, M. J.; Wehmeyer, K. R.; Hynd, B. A.; Eichhold, T. H.; Clear, R. M.; Coggeshall, C. W.; Kuhlbeck, D. L. *Agents Actions* **1994**, *41*, 156.
- Laufer, S. A.; Augustin, J.; Dannhardt, G.; Kiefer, W. *J. Med. Chem.* **1994**, *37*, 1894.
- Alvaro-Gracia, J. M. *Rheumatology* **2004**, *43*, i21.
- Feldmann, M.; Maini, R. N. *Nat. Med.* **2003**, *9*, 1245.
- Laufer, S.; Tries, S.; Pelletier, J. P. *Arthritis Rheum.* **2001**, *44*, 2320.
- Inagaki, M.; Tsuri, T.; Jyoyama, H.; Ono, T.; Yamada, K.; Kobayashi, M.; Hori, Y.; Arimura, A.; Yasui, K.; Ohno, K.; Kakudo, S.; Koizumi, K.; Suzuki, R.; Kawai, S.; Kato, M.; Matsumoto, S. *J. Med. Chem.* **2000**, *43*, 2040.
- Wagner, A. W.; Banholzer, R. *Chem. Ber.* **1963**, *96*, 1177.
- Abramovitch, R. A.; Azogu, C. J.; McMaster, I. T. *J. Am. Chem. Soc.* **1969**, *91*, 1219.
- Abramovitch, R. A.; Azogu, C. J.; McMaster, I. T.; Vanderpool, D. P. *J. Org. Chem.* **1978**, *43*, 1218.
- Rabai, J.; Kapovits, I.; Jalsovszky, I.; Argay, Gy.; Fulop, V.; Kalman, A.; Koritsanszky, T. *J. Mol. Struct.* **1996**, *382*, 13.
- Sang, X.; Du, X. K.; Kadow, J. F. Benzo- and Azabenzodithiazole Compounds. U.S. Patents 7,087,621, 2006 and 0,101,646, 2005.
- Shoichet, B. K. *Nature* **2004**, *432*, 862.
- Kurumbail, R. G.; Stevens, A. M.; Gierse, J. K.; McDonald, J. J.; Stegeman, R. A.; Pak, J. Y.; Gildehaus, D.; Miyashiro, J. M.; Penning, T. D.; Seibert, K.; Isakson, P. C.; Stallings, W. C. *Nature* **1996**, *384*, 644.
- (a) Kuntz, I. D.; Blaney, J. M.; Oatley, S. J.; Langridge, R.; Ferrin, T. E. *J. Mol. Biol.* **1982**, *161*, 269; (b) Kuntz, I. D. *Science* **1992**, *257*, 1078; (c) Shoichet, B. K.; Stroud, R. M.; Santi, D. V.; Kuntz, I. D.; Perry, K. M. *Science* **1993**, *259*, 1445.
- Kast, R. E. *Biomed. Pharmacother.* **2000**, *54*, 168.
- Endres, S.; Whitaker, R. E.; Ghorbani, R.; Meydani, S. N.; Dinarello, C. A. *Immunology* **1996**, *87*, 264.
- Mansilla-Rosello, A.; Ferron-Orihuela, J. A.; Ruiz-Cabello, F.; Garrote-Lara, D.; Fernandez-Mondejar, E.; Delgado-Carrasco, M. L. *J. Surg. Res.* **1997**, *67*, 199.
- (a) Santucci, L.; Fiorucci, S.; Giansanti, M.; Brunori, P. M.; Di Matteo, F. M.; Morelli, A. *Gut* **1994**, *35*, 909; (b) Appleyard, C. B.; McCafferty, D. M.; Tigley, A. W.; Swain, M. G.; Wallace, J. L. *Am. J. Physiol.* **1996**, *270*, G42.
- Nalbant, S.; Akmaz, I.; Kaplan, M.; Avsar, K.; Solmazgul, E.; Sahan, B. *Clin. Exp. Rheumatol.* **2006**, *24*, 361.
- Kumar, S.; Boehm, J.; Lee, J. C. *Nat. Rev. Drug Disc.* **2003**, *2*, 717.
- Jones, G.; Willett, P.; Glen, R. C.; Leach, A. R.; Taylor, R. *J. Mol. Biol.* **1997**, *267*, 727.
- Jensen, A. E.; Knochel, P. *J. Organomet. Chem.* **2002**, *653*, 122.